Vacuum 234 (2025) 114091

Contents lists available at ScienceDirect

Vacuum

journal homepage: www.elsevier.com/locate/vacuum

Design status of the vacuum system of IFMIF-DONES particle accelerator

César Caballero Pérez [a,*], Marcelo Juni Ferreira [b], Volker Hauer [c], Iván Podadera [a], Anderson Sabogal [d], Daniel Sánchez Herranz [a], Claudio Torregrosa [a]

[a] IFMIF-DONES Consortium, Escúzar, 18130, Granada, Spain
[b] ESS, Lund, Sweden
[c] KIT, Karlsruhe, Germany
[d] University of Granada, Escúzar, 18130, Granada, Spain

ARTICLE INFO

Handling Editor: Oleg Malyshev

Keywords:
Vacuum
Particle accelerators
Large-scale vacuum solutions

ABSTRACT

The International Fusion Materials Irradiation Facility-DEMO Oriented Neutron Source (IFMIF-DONES) will be an installation capable of qualifying materials for use in future fusion power reactors. To do so, a linear accelerator will deliver high-intensity deuteron beam to a liquid Li loop, creating a flow of neutrons that will produce material damage equivalent to that expected in a fusion reactor. The vacuum system must maintain high vacuum conditions during operation with high reliability. For this reason, a careful study of the vacuum has been assessed and implemented in the accelerator project. Vacuum simulations have been performed in order to have a first estimation of the expected pressure profile, and documentation is being produced to standardize the subsystem. Additionally, valuable knowledge from the prototype installation, IFMIF/Engineering Design and Engineering Validation Activities (EVEDA), is being taking into account in engineering design activities. Moreover, two vacuum related prototypes are being manufactured; the Multipurpose Vacuum Accident Scenarios (MuVacAS) prototype will enable experimental studies of air inrush in the last section of the accelerator; and the Quick Disconnecting System (QDS) prototype is being developed to study the feasibility of the remote handling of the interface located between the accelerator beam line and the target chamber. The paper presents the status of the design of the vacuum subsystem of the accelerator and discusses the future challenges.

1. Introduction

This article provides a comprehensive overview of the vacuum system for the International Fusion Materials Irradiation Facility-DEMO Oriented Neutron Source (IFMIF-DONES), detailing its design, key components, and associated challenges. It also discusses vacuum modelling and its various gas sources influencing the vacuum conditions. Additionally, a review of the prototypes being developed to validate the system's reliability and effectiveness is included. This article aims to highlight the systems supporting the operation of IFMIF-DONES and their role in advancing fusion research.

1.1. IFMIF-DONES

The IFMIF-DONES is an advanced neutron irradiation facility designed to test and qualify materials for fusion reactors [1]. It plays a crucial role in the European strategy for achieving fusion-based electricity generation. The primary objective of IFMIF-DONES is to examine how materials behave under neutron irradiation, replicating the nuclear conditions expected in the DEMO reactor's first wall, which is intended to succeed ITER. This facility is essential for the design, licensing, and safe operation of DEMO and subsequent fusion power plants.

IFMIF-DONES will provide a vital neutron source, capable of generating neutron fluxes at an energy level of 40 MeV. It will produce a broad energy distribution to simulate the neutron spectrum typical of a deuterium-tritium (D-T) fusion reactor through Li (d,xn) nuclear stripping reactions. The design of IFMIF-DONES is aimed at a minimum operational lifespan of 30 years, with 20 years dedicated to irradiation experiments operating continuously in three shifts. The facility targets an average operational availability of 70 % annually, or 75 % during

This article is part of a special issue entitled: EVC-17/ECOSS-37 published in Vacuum.

* Corresponding author.
E-mail addresses: cesar.caballero@ifmif-dones.es (C.C. Pérez), Marcelo.JuniFerreira@ess.eu (M.J. Ferreira), volker.hauer@kit.edu (V. Hauer), ivan.podadera@ifmif-dones.es (I. Podadera), anderson.sabogal@ifmif-dones.es (A. Sabogal), daniel.sanchez@ifmif-dones.es (D.S. Herranz), claudio.torregrosa@ifmif-dones.es (C. Torregrosa).

https://doi.org/10.1016/j.vacuum.2025.114091
Received 26 September 2024; Received in revised form 16 January 2025; Accepted 27 January 2025
Available online 31 January 2025

scheduled operation periods.

Additionally, the International Fusion Materials Irradiation Facility Engineering Validation and Engineering Design Activities (IFMIF/EVEDA) is developing a comprehensive engineering design for IFMIF and gathering the necessary data to inform future decisions regarding the construction, operation, exploitation, and decommissioning of the neutron source [2]. This is an international project that it is being carried out with the collaboration of Japan and Europe. Within the framework of this project, the Linear IFMIF Prototype Accelerator (LIPAc) oversees the validation activities of the particle accelerator, hence, also the vacuum system. A lot of feedback has been gained from its design and it has been applied to the vacuum system of IFMIF-DONES.

1.2. Particle accelerator

The IFMIF-DONES accelerator, with 100 m of length, is designed to generate, accelerate, and transport the D+ beam with the necessary characteristics to the lithium target [3]. The D+ beam is produced by an Electron Cyclotron Resonance ion source and extracted and accelerated in continuous wave (CW) mode up to 100 keV. A Low Energy Beam Transport (LEBT) section then guides the deuteron beam from the source to a Radio Frequency Quadrupole (RFQ), which is designed to bunch and accelerate the beam from 100 keV to 5 MeV [4]. The beam coming out of the RFQ is directed into a Medium Energy Beam Transport (MEBT) section [5], providing the interface between the RFQ and the Superconducting Radio Frequency Linac (SRF LINAc) [6] that gives the particles their final speed being 40 MeV. Following the Linac, a High Energy Beam Transport (HEBT) [7] line guides the deuteron beam toward the target, using magnetic elements to shape it into a rectangular footprint that impacts the lithium jet. Lastly the Radiation Interface Zone (RIZ) and the Target Interface Room (TIR) section act as the interface between the target and the beamline. The final beam power of IFMIF-DONES particle accelerator is 5 MW.

2. Vacuum system

The goal of the vacuum system of IFMIF DONES particle accelerator is to maintain ultra-high vacuum levels in the beam path to ensure efficient beam transport with low energy dissipation and to allow the high voltage gradient on the superconducting cavities during the lifetime of the operation. The vacuum system is divided into the same sections as the accelerator itself, and two of these sections have been further divided into subsections. SRF LINAc has been divided into five subsections, one per cryomodule. The HEBT has been divided into five subsections as well, the first section (S1) being right after the last cryomodule, followed by the Dipole Junction, where the accelerator line is divided in two, the beam dump section and the section two (S2) of HEBT. Lastly there is section three (S3) just before the RIZ/TIR modules. Fig. 1 shows all the sections and subsections of the particle accelerator.

One aspect of the linear accelerator is that high beam losses are expected at key points, which produce high radiation, its specific locations are specified in the following sections. To avoid the radiation, all the high vacuum equipment has no controllers or electronics drive units inside the vault, and the primary pumping system and the rest of the controllers are located in the room next to the vault. Pumping systems have been tested and verified in LIPAc, however they received less doses than the ones expected in IFMIF-DONES. In the next sections, the pumping speed of high vacuum systems are specified for Nitrogen.

Another safety aspect is that all sections of the accelerator are equipped with burst disks. This is a safety device used in vacuum chambers and other pressurized systems that is comprised of a thin, pressure-sensitive membrane designed to rupture at a specific pressure threshold, thereby providing a controlled path for pressure release and preventing potential damage to the chamber or surrounding equipment.

2.1. Injector

LEBT consists of two vacuum chambers separated by a gate valve. The first chamber, connected to the upstream source, marks the start of the accelerator line. The second chamber is a copper cone directly connected to the RFQ via a helicoflex junction, with an internal interface orifice of 17 mm between the injector and the RFQ. The required pressure level of the Injector is to be lower than 5×10^{-7} mbar. The 3D model is shown in Fig. 2 and a simplified schematic is shown in Fig. 3.

To maintain the required vacuum level, turbo molecular pumping (TMP) systems are installed along the LEBT. The first TMP, with a pumping speed greater than 2800 l/s, is installed on the vacuum chamber between the two solenoids, while a second pump is installed on the copper cone with a lower pumping speed of at least 150 l/s. During the injector commissioning phase, a third TMP is installed on the diagnostic vacuum chamber, replacing the RFQ in this stage.

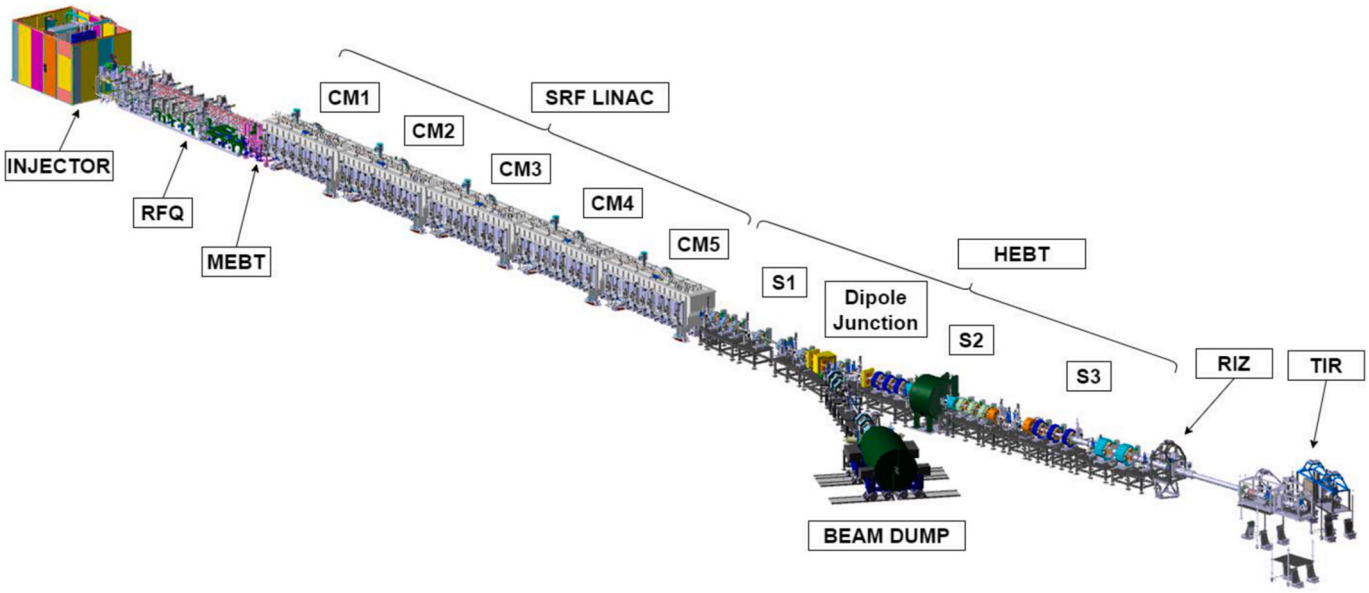

Fig. 1. IFMIF DONES vacuum sections.

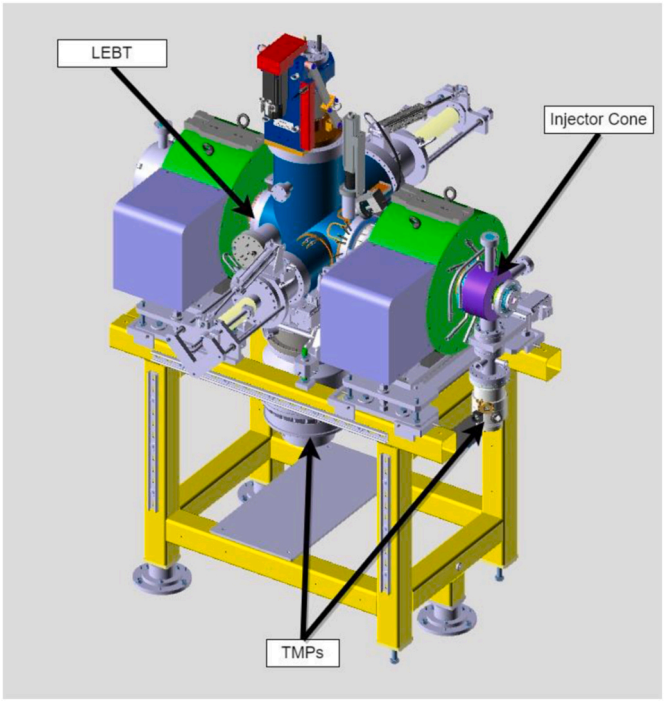

Fig. 2. Injector 3D model.

Each pumping system adheres to the same operational principles, with each TMP equipped with its own primary pump (PP) due to significant differences in pumping speeds. The primary pumps used in this section are multi-root pumps of 60 m^3/h and 7 m^3/h respectively with the TMPs.

Each of the vacuum chambers is fitted with a burst disk. Additionally, the first chamber of the injector has a connection for injecting H_2 or Kr to counteract space charge effects of the beam at low energies, in accelerators, especially at low energies where particle velocities are relatively slow, these space charge effects can lead to beam spreading, distortion, or even instability, reducing the accelerator's performance and beam quality. To compensate it a background of opposite charges is introduced near the beam path.

Several valves are installed throughout this section. Each pumping group features a gate valve to separate the high vacuum pumps from the chamber, an automatic valve for isolating the TMP, an automatic valve for injecting Ar or N_2 for venting purposes located just after the TMP, and a hand valve for connecting a He leak detector situated between the TMP and the primary pump.

Instrumentation for this section include Pirani (PI) and Penning (PE) gauges on each vacuum chamber. The first chamber also contains a Residual Gas Analyzer (RGA) connected to the chamber with a hand valve. Additionally, Pirani and Penning gauges are placed after each TMP and before the gate valve of each pumping group.

2.2. Radio Frequency Quadrupole

The Radiofrequency Quadrupole (RFQ) is a four-vane copper cavity, 9.8 m in length, divided into 18 modules [4]. Each module features two sets of four lateral openings for cavity pumping, RF injection, and tuning. The RFQ vacuum system includes ten TMPs, necessary due to the high beam losses expected in this section. Beam losses are higher at the beginning, so four TMPs are placed in the first two modules, the third module is left spare, and another four are placed in the next two modules. The remaining two TMPs are installed after the couplers. The required pressure level of the RFQ is to be lower than 5×10^{-7} mbar. The 3D model is shown in Fig. 4 and a simplified schematic is shown in Fig. 5.

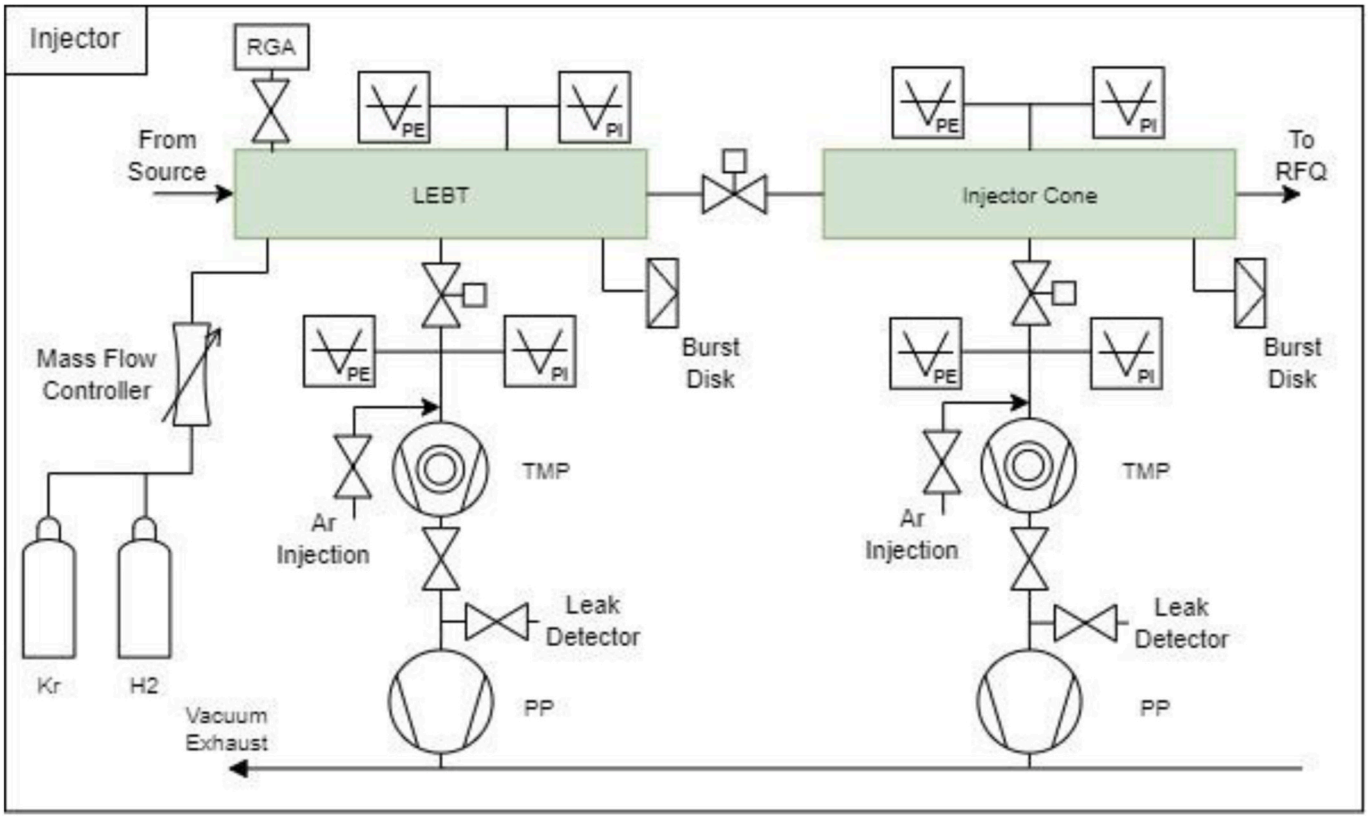

Fig. 3. Injector vacuum system simplified schematic.

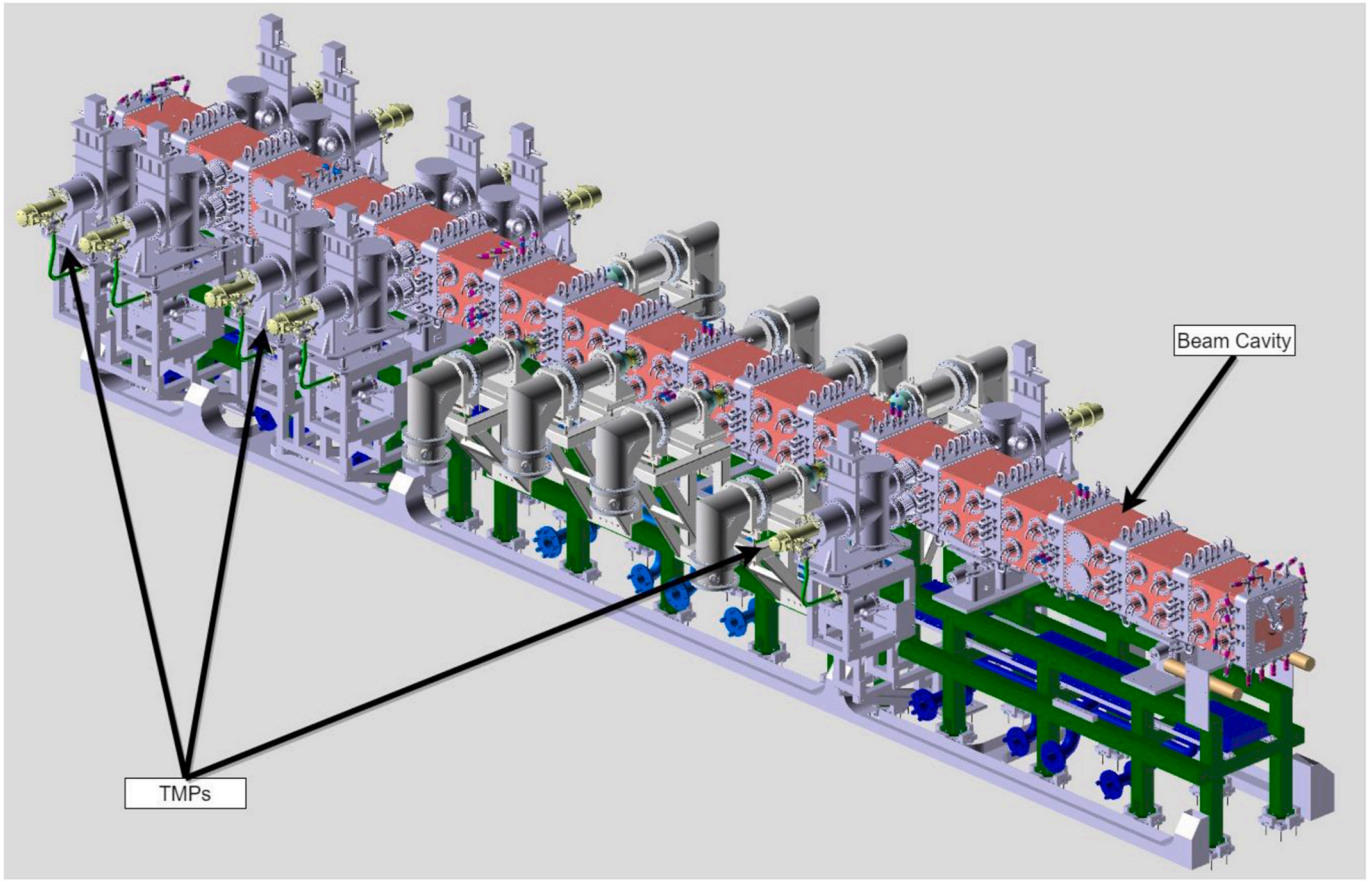

Fig. 4. RFQ 3D model.

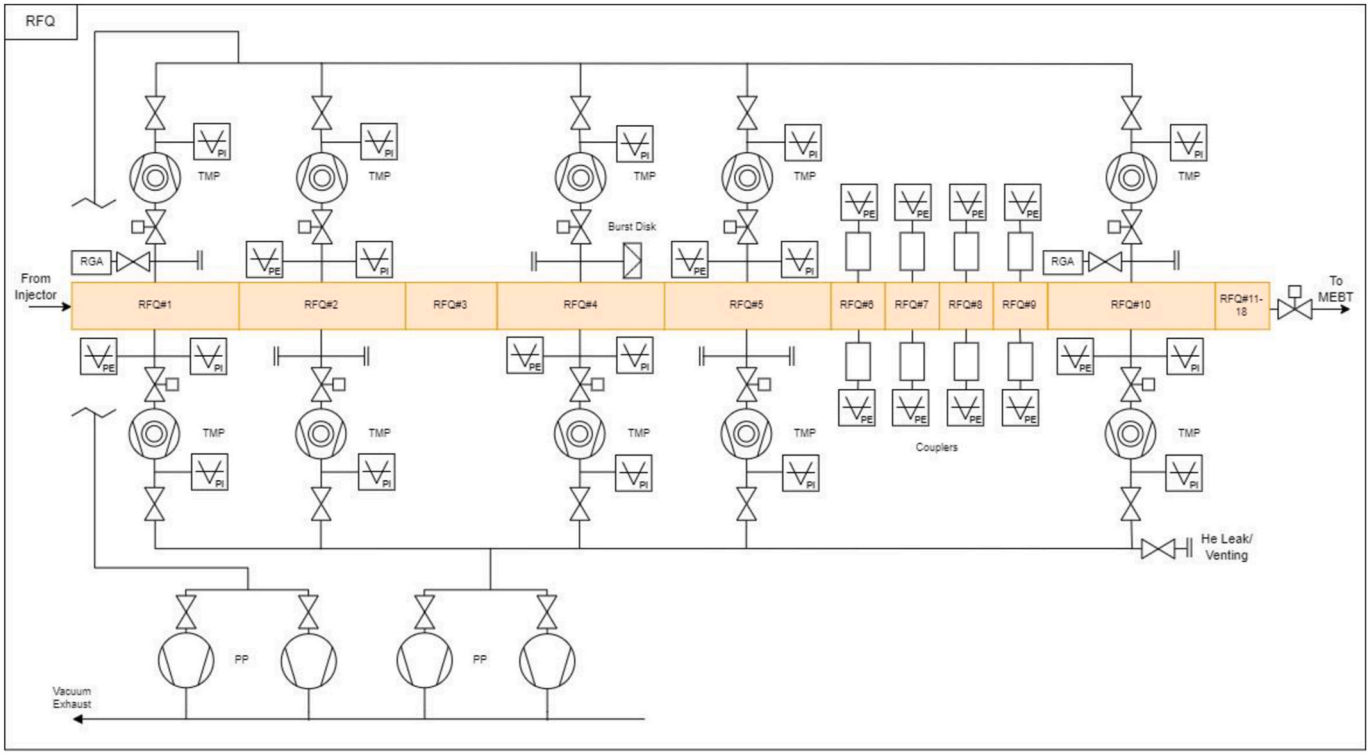

Fig. 5. RFQ vacuum system simplified schematic.

Each side of the RFQ hosts a set of five TMPs, sharing the same output manifold and all with a pumping speed of at least 700 l/s. Two parallel primary pumps, multi-roots, are connected to each output manifold, each of 500 m^3/h.

Several valves are essential for the RFQ vacuum system. A sector gate valve is positioned at the end of the section, and each TMP has its own gate valve. Automatic valves isolate each TMP from the output manifold, and the primary pumps can also be isolated for maintenance without losing vacuum. The RFQ cavity has plug ports for injecting argon and nitrogen, both equipped with manual valves, along with a hand valve for connecting a helium leak detector. Each RGA also has a hand valve.

Instrumentation ports are not directly connected to the RFQ copper cavity. Instead, a cylindrical adaptor is placed after each gate valve, and it has ports to accommodate different pressure sensors. Alternating Pirani and Penning gauges are connected to these flanges, totaling five of each. Each coupler is expected to have a Penning gauge, adding ten more. A Pirani gauge is installed at the outlet of each TMP. There are two RGAs in the RFQ, one at the beginning and one at the end of the cavity.

In the IFMIF/EVEDA project in Japan, LIPAc, the vacuum system differs by utilizing two sets of five cryopumps with the same distribution. However, feedback from operation and maintenance has led to a decision to simplify this system with a TMP configuration.

2.3. Medium Energy Beam Transport

The MEBT reliably transports and matches the beam from the RFQ to the input of the first cryomodule of the SRF [5]. The MEBT features two electroplated copper buncher cavities and two scraper cavities, where beam losses are anticipated, producing a dose of radiation to the surrounding components of 1 Gy/h. Its vacuum system includes three TMPs of 510 l/s and one Non-Evaporable Getter (NEG) pump of 500 l/s, all connected to an output manifold linked to two parallel multi-roots pumps of 100 m^3/h. The required pressure level of the MEBT is to be lower than 5×10^{-8} mbar. The 3D model is shown in Fig. 6 and a simplified schematic is shown in Fig. 7.

To isolate each high vacuum pump from the MEBT cavity, gate valves are employed, with an additional sector gate valve at the end of the section. Automatic valves are situated at the outputs of the TMPs, and each primary pump also has two automatic valves. Hand valves are provided for argon or nitrogen injection, located in the helium leak detector plug and the RGA. A plug is available for pumping with a Slow Pumping System (SPS), used during the initial pump-down when the cryomodules are installed. The SPS is necessary to allow a particle free vacuum when the cryomodules are installed, its functions are explained in the next section.

Instrumentation for this section includes two Penning gauges and one Pirani gauge directly connected to the cavity, a Pirani gauge after each TMP, and an RGA at the end of the section.

2.4. Superconducting Radio Frequency LINAc

The SRF LINAc vacuum system needs to satisfy the particle free requirement for SRF cavities, and it is organized into five subsections, each associated with one cryomodule. The first four subsections include

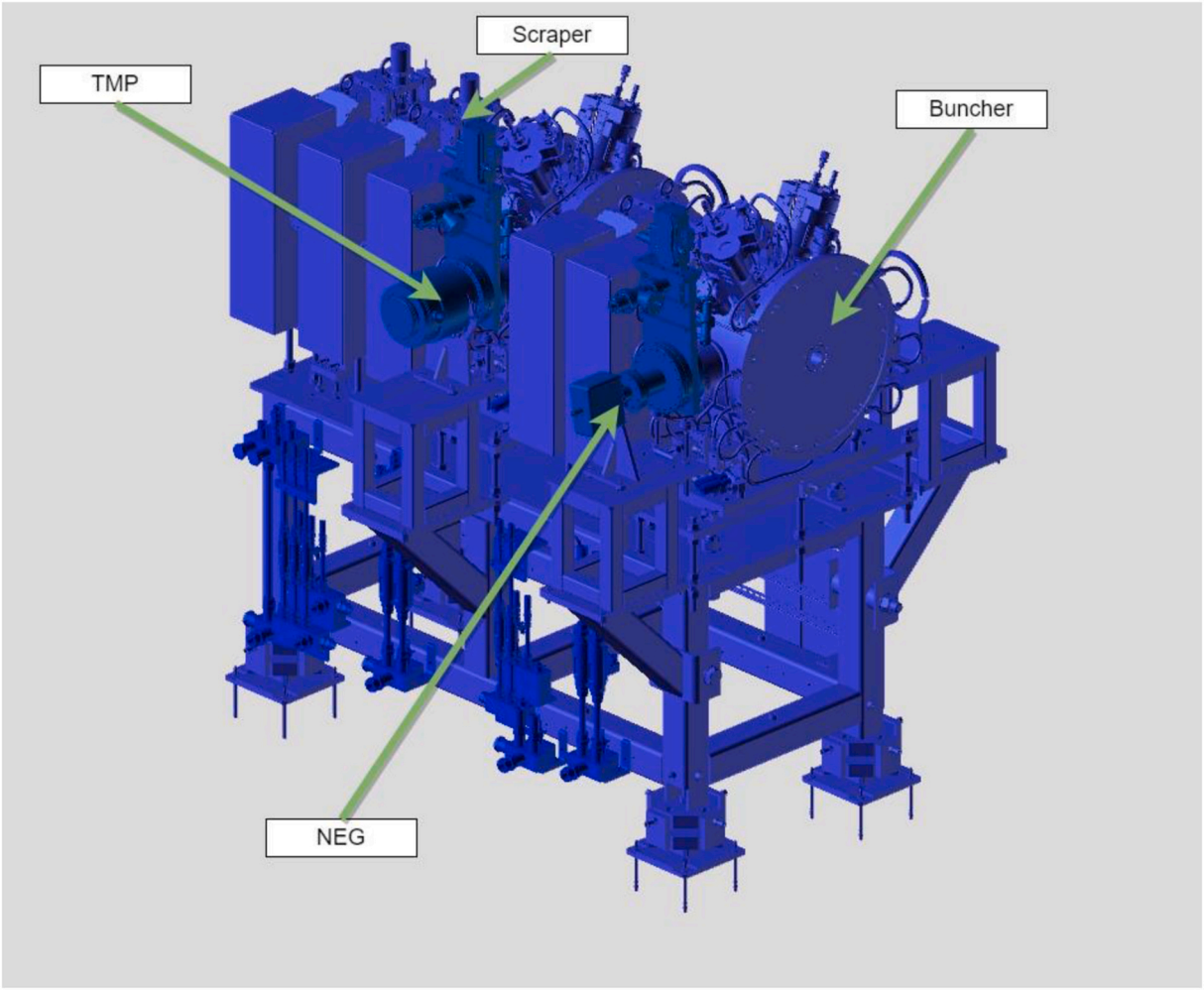

Fig. 6. MEBT 3D model.

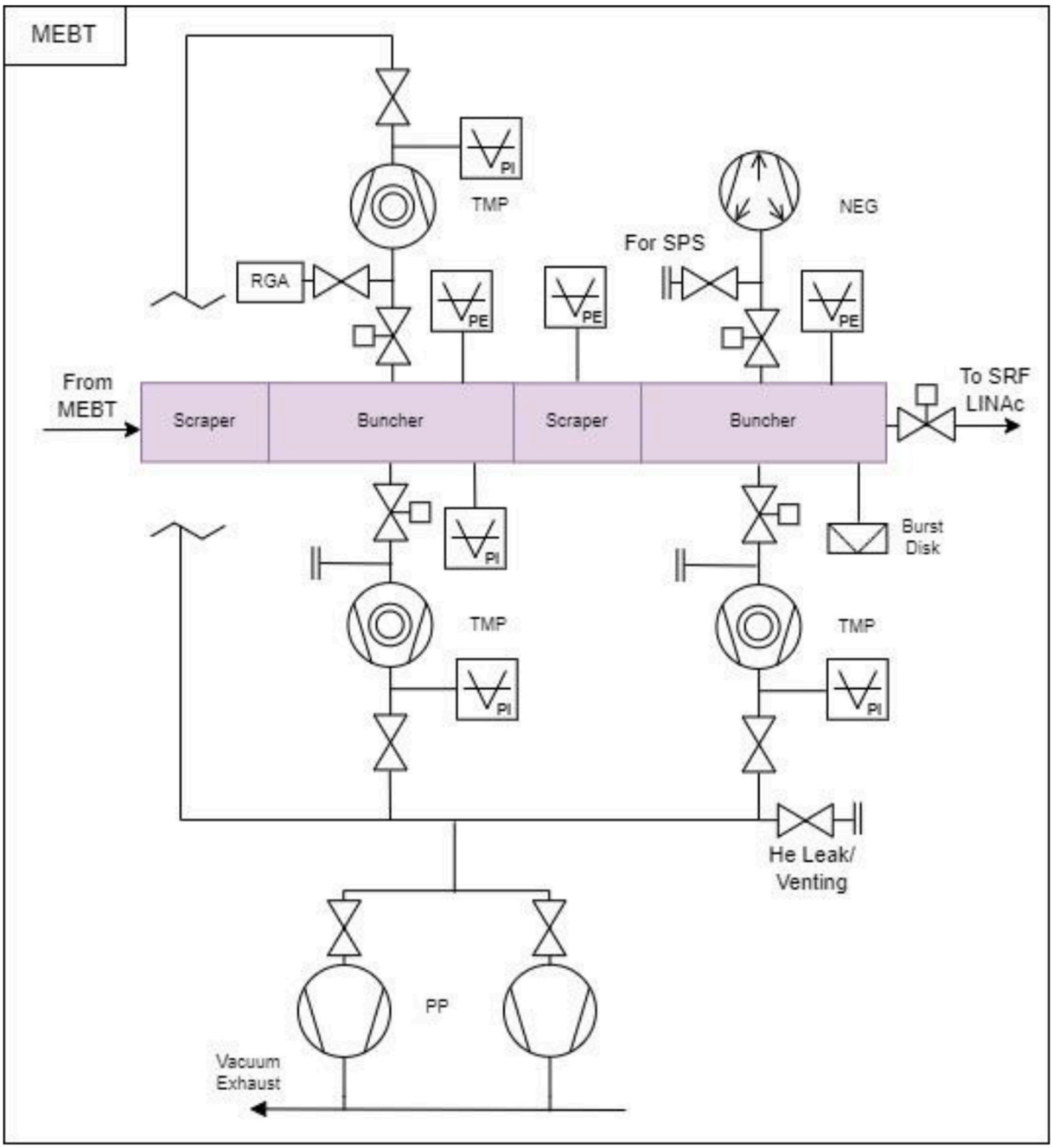

Fig. 7. MEBT vacuum system simplified schematic.

both the beam cavity of the cryomodule and a warm section that separates each cryomodule, whereas the fifth subsection lacks a warm section. Besides the beam cavity vacuum, the cryomodules also have an independent insulation vacuum managed by the vacuum system. The beam vacuum of the SRF will be on cryogenic temperature with a pressure bellow $1x10^{-9}$ mbar, and the insulation vacuum below 10^{-4} mbar at warm, and below 10^{-7} mbar at cold. The vacuum limit of the insulation vacuum is dictated by the amount of heat exchanged of the residual gas and the external tank at room temperature. The 3D model is shown in Fig. 8 and a simplified schematic is shown in Fig. 9.

There are three types of cryomodules, differing in the number of cavities. The first, second, and third cryomodules are unique, while the fourth and fifth are identical to the third.

For the beam cavity vacuum, each cryomodule has a port for connecting a slow pumping system trolley to satisfy particle free requirement (no turbulence) to perform the pump-down of the beam cavity from atmosphere pressure to molecular regime below 10^{-4} mbar.

The insulation vacuum is managed by a pair of TMPs of 300 l/s connected to the thermal shield of the cryomodules, aiming for insulation pressure to avoid heat exchange with the superfluid helium cooling the SRF cavities. These pumps are supported by a pair of multi-roots pumps of 60 m^3/h located in the adjacent room to the vault, responsible for roughing and backing the TMPs. The main goal of the system is to pump helium, in case of a leak that is developed on the inner tank of pipes during the life of the cryomodule operation.

Warm sections are placed after each cryomodule (except the last one), housing diagnostic devices and a NEG pump of 210 l/s. These sections also have a plug for connecting the SPS if needed for maintenance purposes and a burst disk for safety.

Regarding the valves of this section, a sector gate valve is located

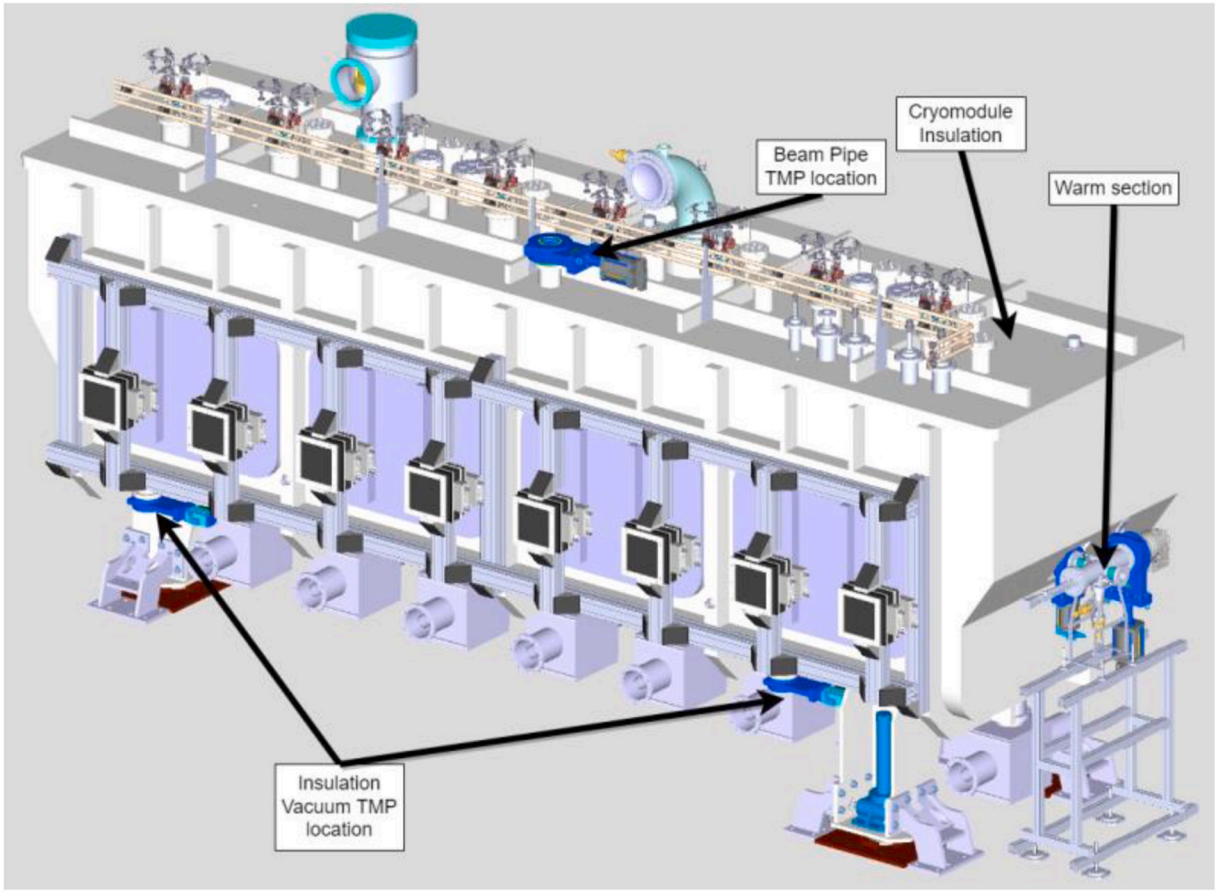

Fig. 8. SRF LINAc 3D Model (SPS not shown in the picture).

after each warm section, or after the fifth cryomodule itself. Gate valves are installed at each pumping port of the cryomodule, the insulation, the beam cavity, and the warm sections. Automatic valves are placed at the outlets of the TMPs and the inlets of the primary pumps.

Instrumentation varies with each cryomodule type. The first cryomodule has eight Penning gauges, the second has eleven, and the third to fifth have nine each; it depends on the number of couplers it possesses. Additionally, each warm section contains a Penning and a Pirani gauge, a Pirani gauge is located at the outlet of the insulation TMPs, and, lastly, a Penning gauge is placed on the thermal insulation of each cryomodule.

The slow pumping system is an independent unit equipped to prevent gas flow from entering the turbulent regime during the pump-down sequence on the cavities beam vacuum, monitored by a mass flow controller. This unit includes a TMP of at least 200 l/s, a multi-roots pump of 60 m^3/h, a Pirani gauge, an RGA, a plug for connecting a helium leak detector, a venting plug connected to another mass flow controller, a pressure switch, and a flow transmitter. Two such units are sufficient to pump down any particle-free cavity of the accelerator.

2.5. High Energy Beam Transport

HEBT section is in charge of guiding the deuteron beam from the exit of the Superconducting Radio Frequency Linac towards the Lithium Target [7,8]. The HEBT section vacuum system is divided into five subsections. It starts with a subsection immediately after the SRF LINAc and carries on to the second subsection called, HEBT dipole junction. In this subsection the beam cavity is divided in two, the HEBT beam dump section and the HEBT section 2. Finally, there is one more subsection before reaching the RIR modules and the TIR. The required pressure level of the RFQ is to be lower than 5×10^{-8} mbar at the interface with the SRF LINAc, as the end pressure, due to the presence of the high gas load coming from the target, will raise it to 1×10^{-5} mbar. High beam losses are expected at the HEBT Main Scraper, producing a dose of radiation to the components of 10 Gy/h. Radiation resistant vacuum components are selected where these high doses are expected, specifically the TMPs and all metal gate valves. Due to the high activation of the HEBT the last sections of it are mainly made of aluminum, which is a lower activation material. The 3D model is shown in Fig. 10 and the simplified schematic is shown in Figs. 11–15.

The vacuum system of HEBT is entirely comprised of TMPs, where all the vacuum stations follow the same design principles, except for the first vacuum station which is a Slow pumping System identical to the one in the SRF LINAc. Each vacuum station has ports for two TMPs of at least 500 l/s, normally one on each side of the accelerator. Each group of two vacuum stations is backed by a pair of primary pumps in parallel of 500 m^3/h. There are two stations per subsection, except for the dipole junction, which only has one.

The valves in each vacuum station are distributed in the same way. Two gate valves are located at the TMPs to be able to isolate them from the HEBT cavity. Automatic valves are placed at the outlets of every TMPs, the inlet of every primary pump and where argon injection is needed for venting. Hand valves are used in the helium leak detector ports in each subsection and in every RGA. There are sector gate valves in each subsection, except for the HEBT beam dump section which lacks it and the dipole junction that has two of them. Finally, at the very beginning of the HEBT there is a pneumatic DN40 safety Fast Isolation Valve (FIV).

Each station cavity is equipped with a Pirani and Penning gauge, also, there are Pirani gauges installed at the outlet of the TMPs. Additionally, there are Penning gauges located in some cavities of the accelerator that are far from the vacuum stations. RGAs are installed in each subsection, except for the dipole junction, while burst disks are

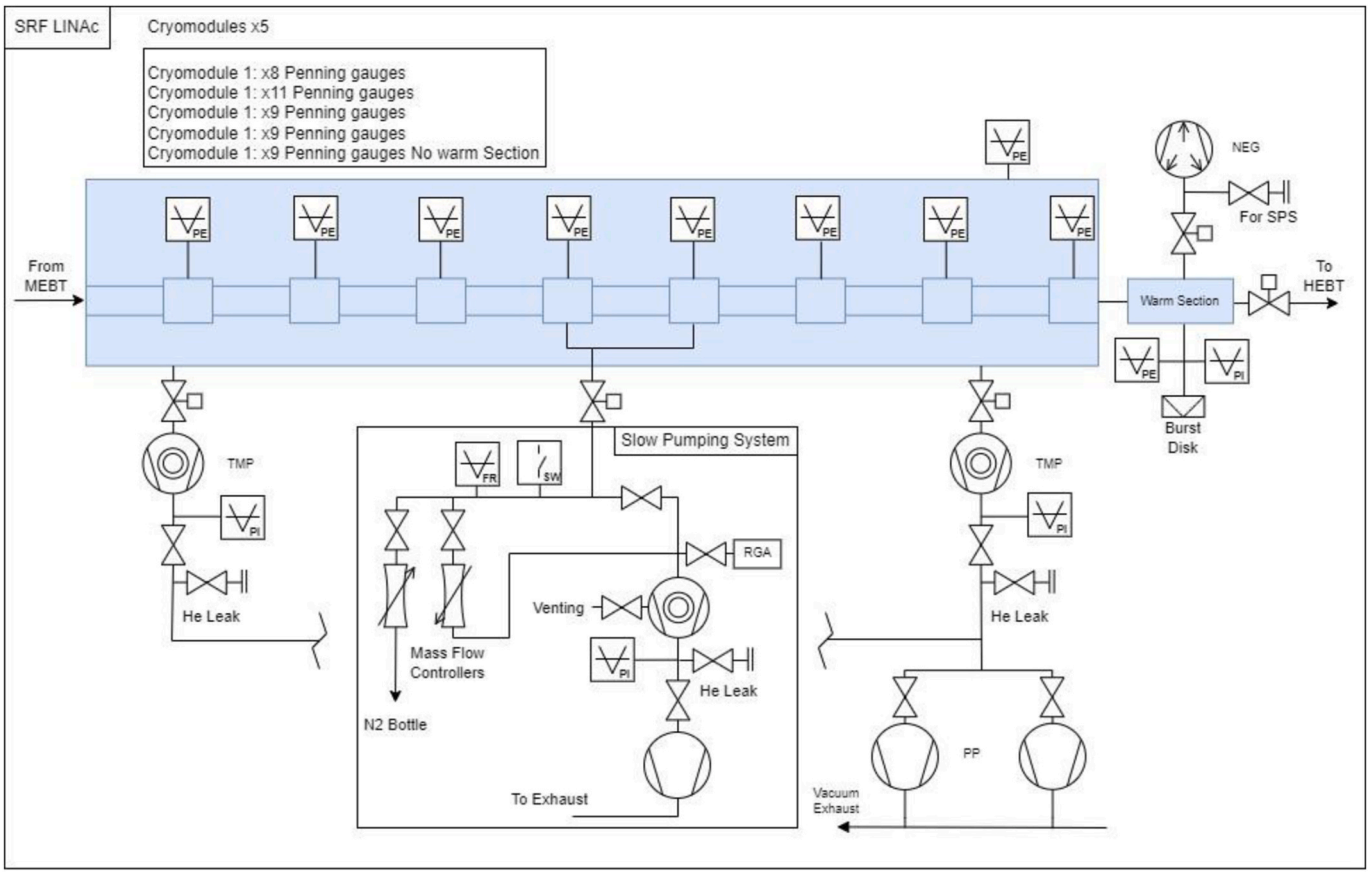

Fig. 9. SRF LINAc vacuum system simplified schematic.

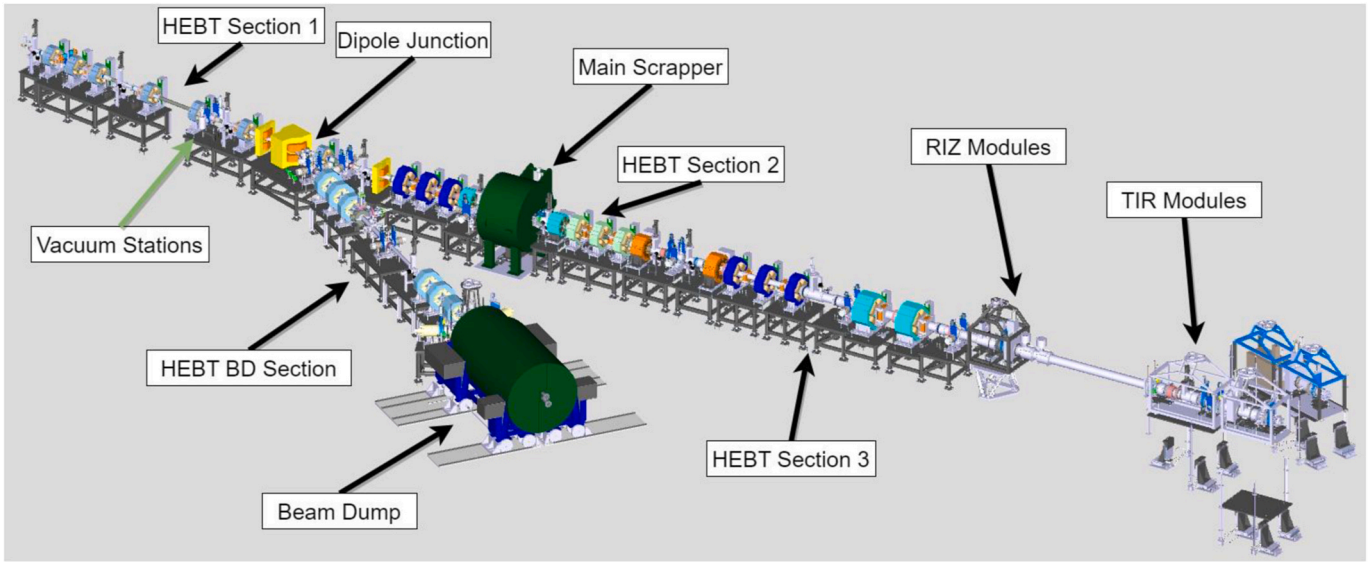

Fig. 10. HEBT and RIZ/TIR 3D model.

installed in all subsections.

The dipole junction section has an additional feature to prevent the entrance of undesired gas load to the SRF LINAc. It is a Cold Trap which is still in conceptual design, it will be a small cryogenic section with an increased internal surface in order to trap all gases coming from the target. The trap will be fed to the surrounding walls of the internal cavity with cryogenic Helium at 60K coming from the cryoplant, whose initial purpose was only to provide cryogenic helium to the cryomodules. Although in design phase, it needs to be validated and verified, the simplicity of the solution and the improvement on the risk of contamination of the SRF LINAc makes this new feature a must-include in the accelerator.

2.6. Radiation Interface Zone and Target Interface Room

The RIZ and TIR sections are the last ones of the accelerator and the

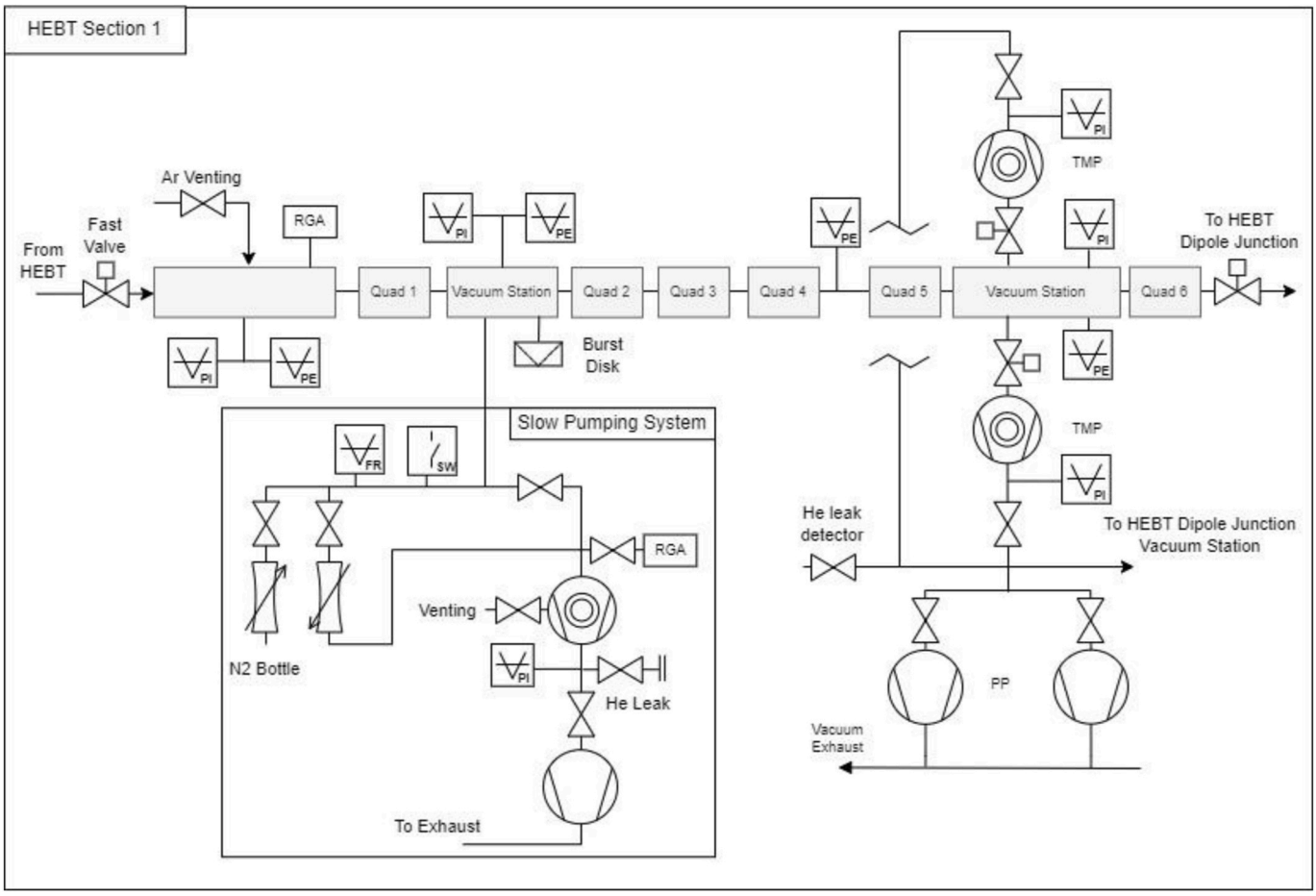

Fig. 11. HEBT 1 vacuum system simplified schematic.

interface with the target. They are still part of the HEBT but are treated separately due to their special characteristics, particularly the high radiation to withstand, the TIR collimator is expected to have a dose of 200 Gy/h to the surrounding components due to beam losses in its scrapers, although radiation resistant vacuum components are selected, the modules are expected to be changed with a set interval of time due to the high radiation dose. The RIR consists of two modules, with the last one being enclosed as a radiation safety measure [9]. In this last module, a FIV is located. Right now, the design expects to place two of them as air inrush accidents can happen in both directions. However, it is expected that experimental results from MuVacAS demonstrate that one FIV will be enough to stop these scenarios (see the later section "Vacuum Prototypes" about the MuVacAS). The TIR is located in the next room, and vacuum-wise, a high gas source coming from the target is expected. Therefore, the only vacuum systems are connections to primary pumps with a high pumping speed, which is to be specified, located in the room above. There are two gate valves in the beam line, one in the first module of the RIR and the others in the first and second module of the TIR. A simplified schematic is shown in Fig. 16.

3. Vacuum modeling

Several studies have been conducted [10,11] to make an initial estimation of the pressure profiles of the IFMIF-DONES linear accelerator. The primary tool used for these studies is Molflow+, a test-particle Monte Carlo (TPMC) code developed by CERN. These studies also included the prototype accelerator LIPAc, as its first section is the same as that of the IFMIF-DONES linear accelerator. The studies performed include:

- Vacuum transient simulation of electric arc in the RFQ of LIPAc
- Metal condensation in beamline components
- Gas adsorption in the cryomodules
- Calculation of the effective pumping speeds of the cryomodules
- Complete simulation of the linear accelerator

3.1. Boundary conditions

The boundary conditions of the simulations are the pumping speeds specified in all the previous sections and the different gas sources that are expected in the particle accelerator beam cavities.

There are six primary sources of gas within the internal vacuum of the accelerator beam line, all of which have been used as boundary conditions for the vacuum modeling. These are the beam neutral flow, which represents the amount of gas that is not converted into beam in the injector; the thermal outgassing, the result of the gas desorption of the material on any vacuum chamber; there are deuterium beam losses whose value depends on each of the sections and it is due to the beam halo hitting the vacuum cavity walls; there are gas injections, Argon in the test chamber and Krypton as space charge compensation in the injector; and, lastly, there is metal evaporation coming from the lithium target, calculated in a following section. All these values have been studied multiple times [10,11]. Table 1 shows the different gas loads in the particle accelerator, while Table 2 shows the different gas compositions expected. The assumed gas spectrum for the thermal outgassing of the components can be seen in Fig. 17.

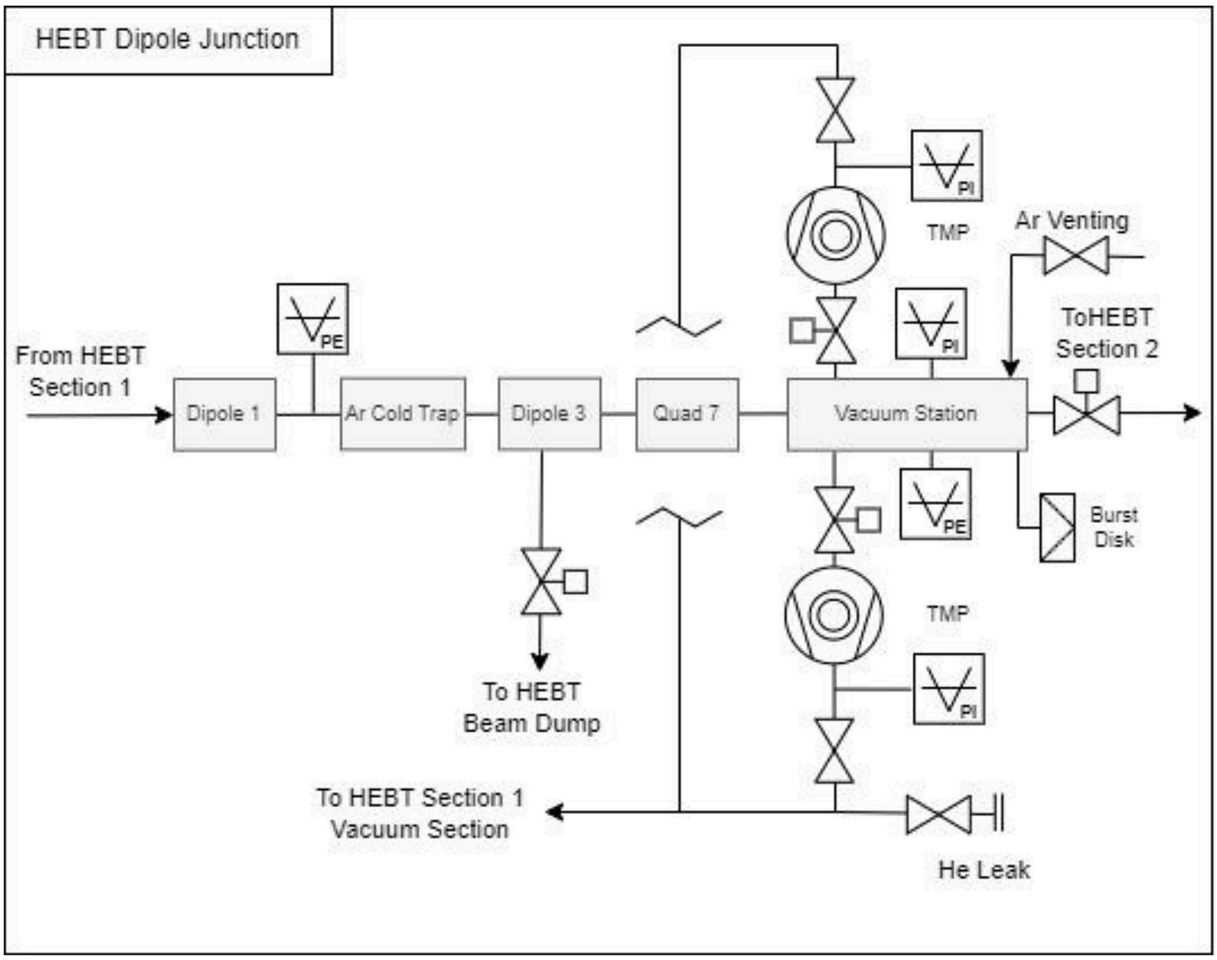

Fig. 12. HEBT dipole junction vacuum system simplified schematic.

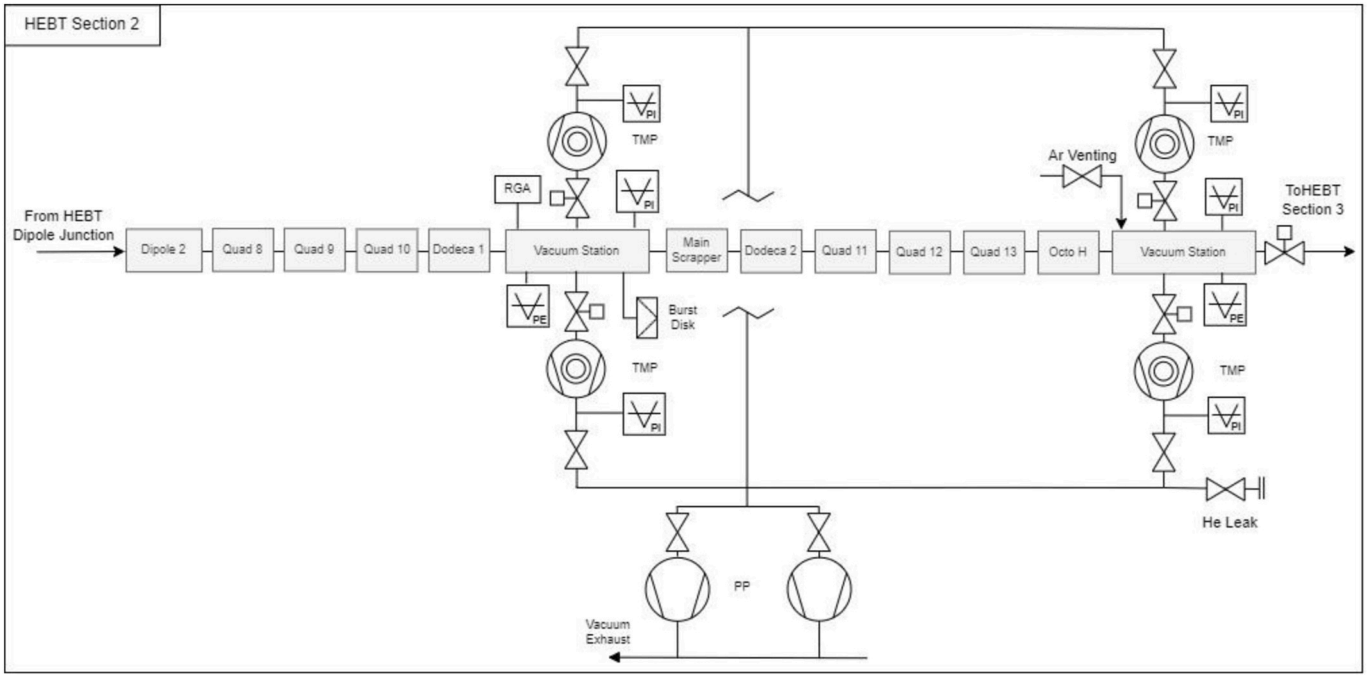

Fig. 13. HEBT 2 vacuum system simplified schematic.

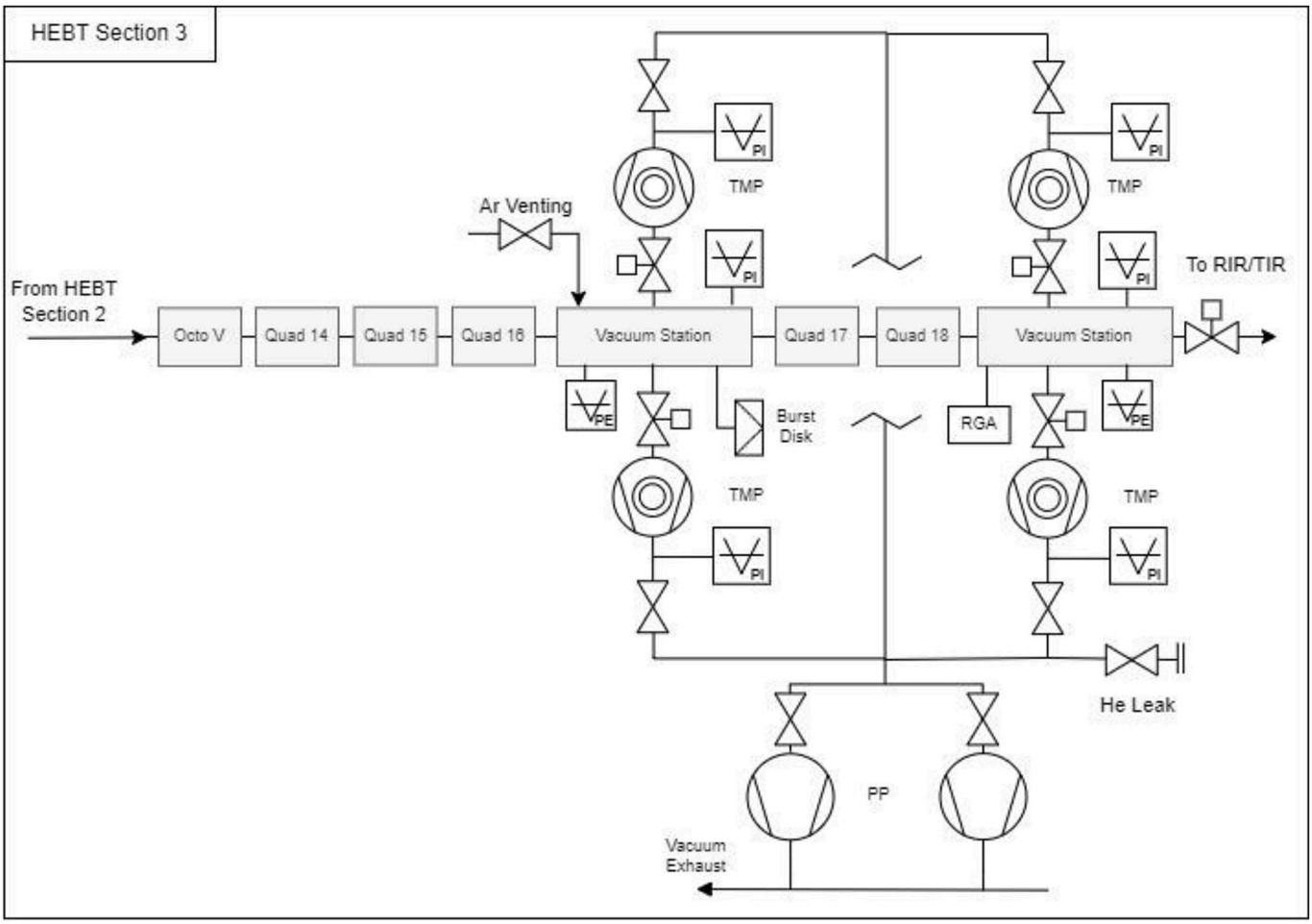

Fig. 14. HEBT vacuum system simplified schematic.

3.2. Transient simulation in RFQ couplers

A transient vacuum study of an electrical discharge at the RFQ of LIPAc was performed using Molflow+. In the RFQ there are eight couplers that make possible Radio Frequency (RF) power to be injected, and they are known to produce electric arcs in the interior during the RF conditioning. However, the relationship between the electric arcs and the pressure readings of the gauges was unclear. The electrical discharge was simulated as a virtual injection of particles in the surface where it is likely to happen. It was found that in the couplers the pressure can rise two orders of magnitude due to these arcs [12]. (See Fig. 18).

3.3. Metal condensation in beam line components

In this simulation, lithium, potassium, and sodium vapor enter the beamline and condense onto components due to lower wall temperatures, while interactions with the beam and residual gas are ignored. The goal is to determine deposition rates on various beamline components near the target.

Separate sub-models were used for lithium, potassium, and sodium, with vapor pressures calculated per established equations [13]. A uniform evaporation rate was assumed across the lithium surface, with a sticking factor of 0.4 to account for partial re-condensation. Sticking factors for other surfaces varied by temperature: components in contact with liquid lithium (570 K) had a sticking factor of zero, beam ducts (323 K) had a factor of 1, and HEBT components (293 K) also had a factor of 1.

The metal layer thicknesses were calculated for each metal over a year of operation using a 1×1 cm grid model. The average impingement rate was determined by distance to the target, then multiplied by the quotient of molar mass and Avogadro's number to yield mass flow density. Calibration was performed by comparing the ratio of adsorbed to total mass flow with the ratio of adsorbed to desorbed particles. Corrected mass flow densities were divided by metal density and adjusted by operational time (340 days).

The thickness of the resulting metal layers is on average 10^{-4} μm per year throughout the accelerator, while near the target they can reach up to 10^{1} μm per year. Results are shown on Fig. 19. Peaks in the graphs indicate areas of higher lithium deposition, caused by reductions in cross-sectional areas at those points. Overall, the vacuum performance will remain unaffected as long as the deposited layer does not significantly increase the total outgassing rate.

3.4. Gas adsorption in cryomodules

Gas adsorption measurements were carried out for carbon monoxide, carbon dioxide, argon, and krypton. Adsorption of hydrogen and deuterium was excluded under the assumption that niobium surfaces were saturated, with minimal diffusion expected due to the low temperature. Argon adsorption was mainly relevant to the last cavity, while krypton adsorption was primarily relevant to the first cavity.

Adsorption of these gases results in particle cluster formation, which then evolves into layered structures. These layers, depending on their thickness, alter the electric field within the cavity. The threshold thickness is considered to be equivalent to four monolayers. The reason for this threshold come from specific tests made in the past, cooling

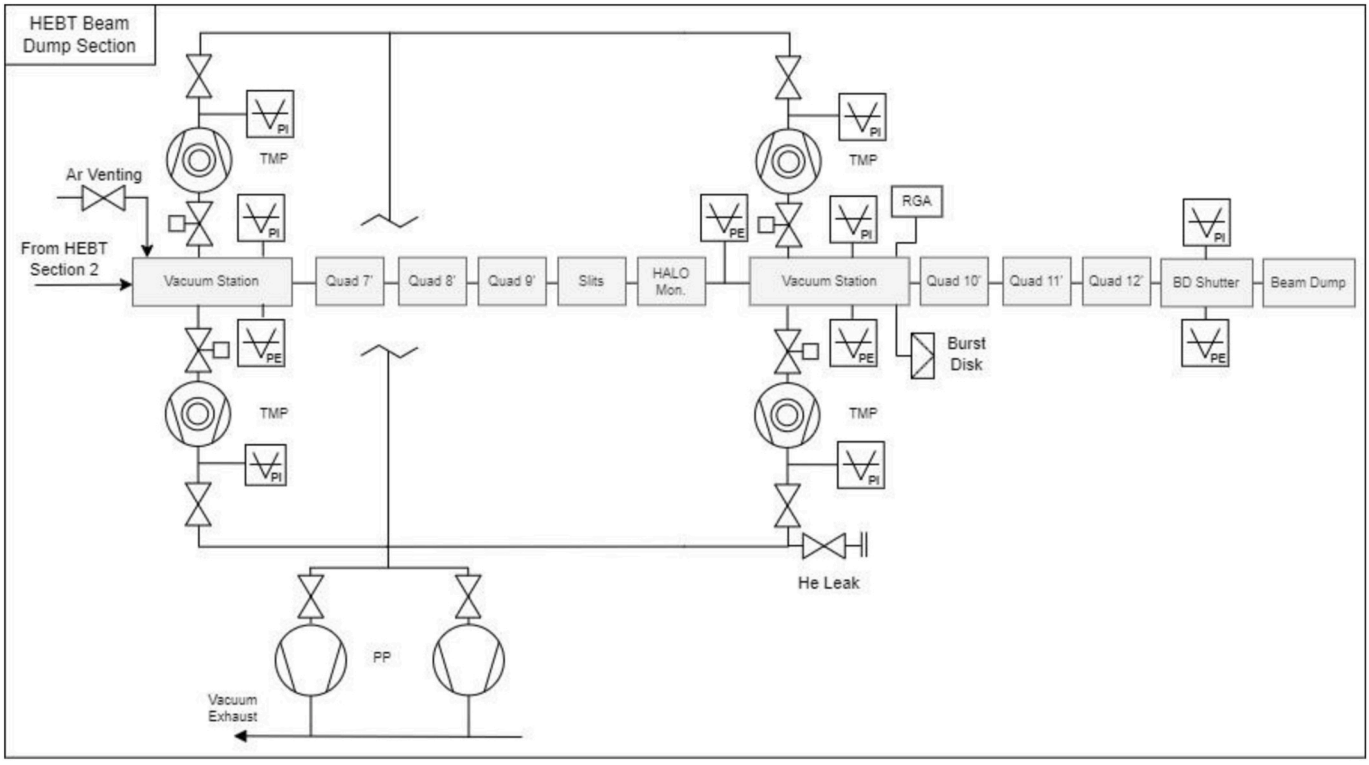

Fig. 15. HEBT BD vacuum system simplified schematic.

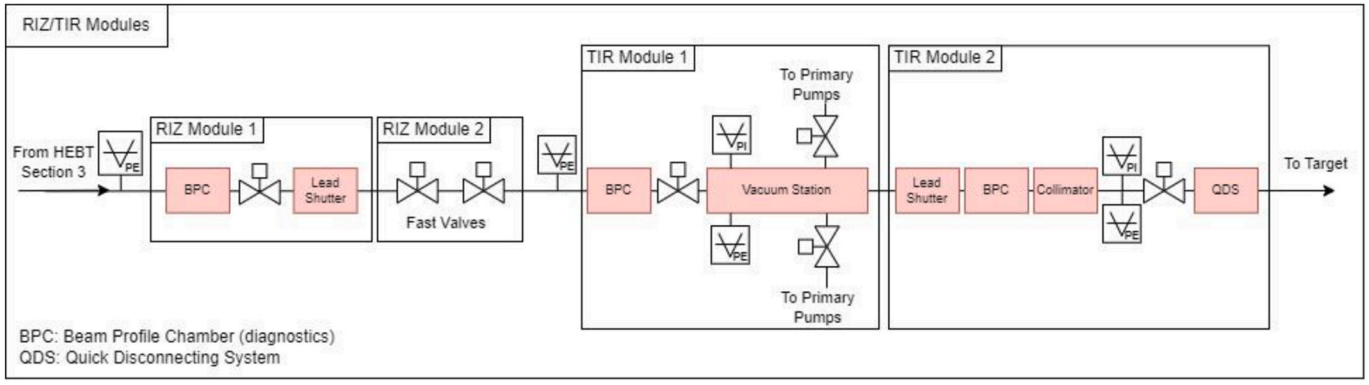

Fig. 16. RIZ/TIR vacuum system simplified schematic.

Table 1
Gas loads in the different subsections of IFMIF-DONES.

	Beam Neutral Flow $\left(\frac{mbar\,l}{s}\right)$	Thermal outgassing $\left(\frac{mbar\,l}{s}\right)$	Beam losses (target) $\left(\frac{mbar\,l}{s}\right)$	Argon injection $\left(\frac{mbar\,l}{s}\right)$	Krypton injection $\left(\frac{mbar\,l}{s}\right)$	Metal evaporation $\left(\frac{mbar\,l}{s}\right)$
LEBT	3.3×10^{-2}	$1.8 \bullet 10^{-6}$	$7.8 \bullet 10^{-3}$	$7.1 \cdot 10^{-3}$	$8.4 \bullet 10^{-3}$	–
RFQ		$1.7 \bullet 10^{-5}$	$1.2 \bullet 10^{-3}$	–	–	–
MEBT		$1.1 \bullet 10^{-5}$	$8.1 \bullet 10^{-7}$	–	–	–
SRF-L		$8.3 \bullet 10^{-6}$	$3.1 \bullet 10^{-5}$	–	–	–
HEBT		$4.0 \bullet 10^{-5}$	$8.7 \bullet 10^{-6}$	–	–	–
LT		$2.0 \bullet 10^{-6}$	$3.3 \bullet 10^{-8}$[a]	–	–	Li $6.5 \bullet 10^{1}$ K $8.6 \bullet 10^{1}$ Na $1.9 \bullet 10^{1}$

[a] Desorption of D2 and HT from the liquid lithium surface at target.

down SRF cavities to find the highest pressure that would not disrupt the RF full power performance [14]. Using simulation-derived adsorption rates and the available surface area in each cavity, the time required to complete one monolayer was calculated.

The geometric inner surface area of the last cavity was determined to be 1.31 m^2, and for the first cavity, it was 0.53 m^2. The technical surface

Table 2
Gas compositions in DONES particle accelerator.

	Composition	Operating press. (mbar)	Operating temp. (K)
Source [9,14]	Kr, D_2	$1\bullet10^{-5}$ D_2 $4\bullet10^{-5}$ Kr	300
LEBT [9, 14]	Kr, D_2 + outgassing	$1\bullet10^{-5}$ D_2 $4\bullet10^{-5}$ Kr	300
RFQ [10, 14]	D_2 + outgassing	$<5\bullet10^{-7}$	290–340
MEBT [11, 14]	D_2 + outgassing	$5\bullet10^{-7}$-$5\bullet10^{-8}$	300
SRF LINAC [12]	D_2 + outgassing	$<5\bullet10^{-8}$	4.4–300
HEBT [13, 14]	D_2 + outgassing	$<5\bullet10^{-8}$ (SRF Side)	300
BD [13, 14]	D_2 + outgassing	$3\bullet10^{-6}$	300
LT [15]	Ar, D_2 + outgassing + Li, Na and K vapor + product of Li/d reaction (H_2, D_2, T_2, He, Be)	$>1\bullet10^{-4}$–$1\bullet10^{-5}$ (at free-surface)	300–570 (at free surface)

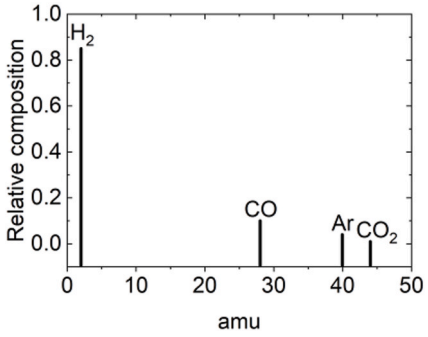

Fig. 17. Assumed gas spectrum for thermal outgassing of components.

area was assumed to be three times greater (3.92 m^2 and 1.58 m^2, respectively). For simplicity, the surface area covered by a single particle was approximated as 1.62×10^{-19} m^2. By dividing the technical surface area by the area occupied by each particle, the particle count per monolayer was estimated to be 2.42×10^{19} for the last cavity and 9.77×10^{18} for the first.

For carbon monoxide and carbon dioxide, particle flux was determined based on the total desorbed gas per unit time, while for argon and krypton, it was calculated from the injected gas flows. The ratio of total gas particle flux to the total desorbed test particles provided a calibration factor for each simulation model, converting gas particles to simulated test particles. By applying this factor to the adsorbed test particles in each cavity, the gas particle flux (in particles per second) was calculated. The time to complete one monolayer was obtained by dividing the monolayer particle count (2.42×10^{19} or 9.77×10^{18}) by the computed gas flux.

The monolayer formation of the first and last cryomodules was calculated to validate the reliability and cleanliness requirements. The time to form one complete monolayer in the first and last cavity was calculated to be 423 days and 278 days, respectively. The last cavity must be warmed up every three years to avoid the adsorption of more than four monolayers.

3.5. *Effective pumping speed of cryomodules*

The effective pumping speed of the cryomodule was calculated using Molflow+ with a sub-model incorporating the HEBT system and the linking tube between the final cavity of the SRF-LINAc and the HEBT. The effective pumping speed at the exit of the last cavity was calculated to be 8.5 l/s, based on nitrogen gas at a temperature of 293 K.

3.6. *Complete simulation of the particle accelerator*

For the complete simulation of the accelerator, TPMC simulations were conducted with Molfow + for particles with molar masses of 4 (primarily from beam losses), 2, 28, and 44 (from thermal outgassing), 40 (from argon injection and thermal outgassing), and 84 (from krypton injection at the Electron Cyclotron Resonance source). Partial pressures were determined by counting the hits on designated surfaces within the models along the beam axis. The total pressure was then obtained by summing these partial pressures. The boundary conditions of this simulation are the different gas sources that will appear in the particle accelerator. Fig. 20 shows the 3D model used in this simulation.

Fig. 21 illustrates the resulting gas pressure profile for the IFMIF-DONES accelerator. This gas pressure profile highlights the distribution of gas loads due to beam losses in the LEBT, RFQ, and SRF-Linac sections. The pressure near the target in the HEBT region is largely influenced by the argon injected at the target, which is necessary to avoid the lithium of the target from boiling or significant vaporization from the lithium surface. Peaks in pressure between the LINAC modules are attributed to temperature changes (warmer sections between the modules) and increased outgassing.

4. Vacuum Prototypes

Several prototypes for the IFMIF-DONES vacuum system are in the process of being built or commissioned. The Multipurpose Vacuum Accident Scenarios (MuVacAS) experimental setup [15] has been developed to test and validate strategies for managing vacuum breach events. A unique aspect of the IFMIF-DONES accelerator is the absence of a separation window between the Target Vacuum Chamber (TVC) and the rest of the accelerator's vacuum line. This design choice arises because the beam's high power and low energy would cause intense power deposition in a thin window, which no material could endure or effectively cool. This design characteristic has specific safety implications; in the event of a Loss of Vacuum Accident (LOVA), incoming air could potentially contact the liquid lithium target or carry activated material through the accelerator line. To address this risk, FSIVs are employed to quickly isolate the target vacuum chamber within 100 ms if a LOVA is detected, acting as a critical safety confinement measure.

To replicate the actual conditions of IFMIF-DONES's vacuum chambers, MuVacAS closely mimics the specifications of the IFMIF-DONES HEBT + TVC setup. It includes modules for conducting various experimental scenarios, such as gas injections (N2, Ar, air, He), demineralized water leaks, sudden air inrush simulations, and a high-speed acquisition system (20 kHz) for data collection and analysis of these events and the effectiveness of safety measures.

The total length of the MuVacAS setup is 28 m, shorter than the 49-m length of the IFMIF-DONES HEBT + TVC chambers due to space constraints. The setup comprises two main sections: Zone A and Zone B. Zone A is scaled down relative to IFMIF-DONES, measuring 14 m instead of 35 m. Zone B, however, maintains a 1:1 scale in both longitudinal and transverse dimensions over its 14 m, covering the area from the TVC to the final meters of the HEBT (downstream of the FIV DN250), which is of particular interest for accident scenarios. Zone A is constructed from aluminum, while Zone B is made of AISI 316L stainless steel, in line with the current HEBT design. The TVC is constructed from 304L stainless steel with a 1 cm wall thickness to evaluate its potential use in the final HEBT design. Fig. 22 shows the 3D model of MuVacAS and Fig. 23 shows a simplified schematic.

The other vacuum related prototype is the Quick Disconnecting System (QDS). This prototype has been developed to experimentally validate the remote handling connection interface present between the

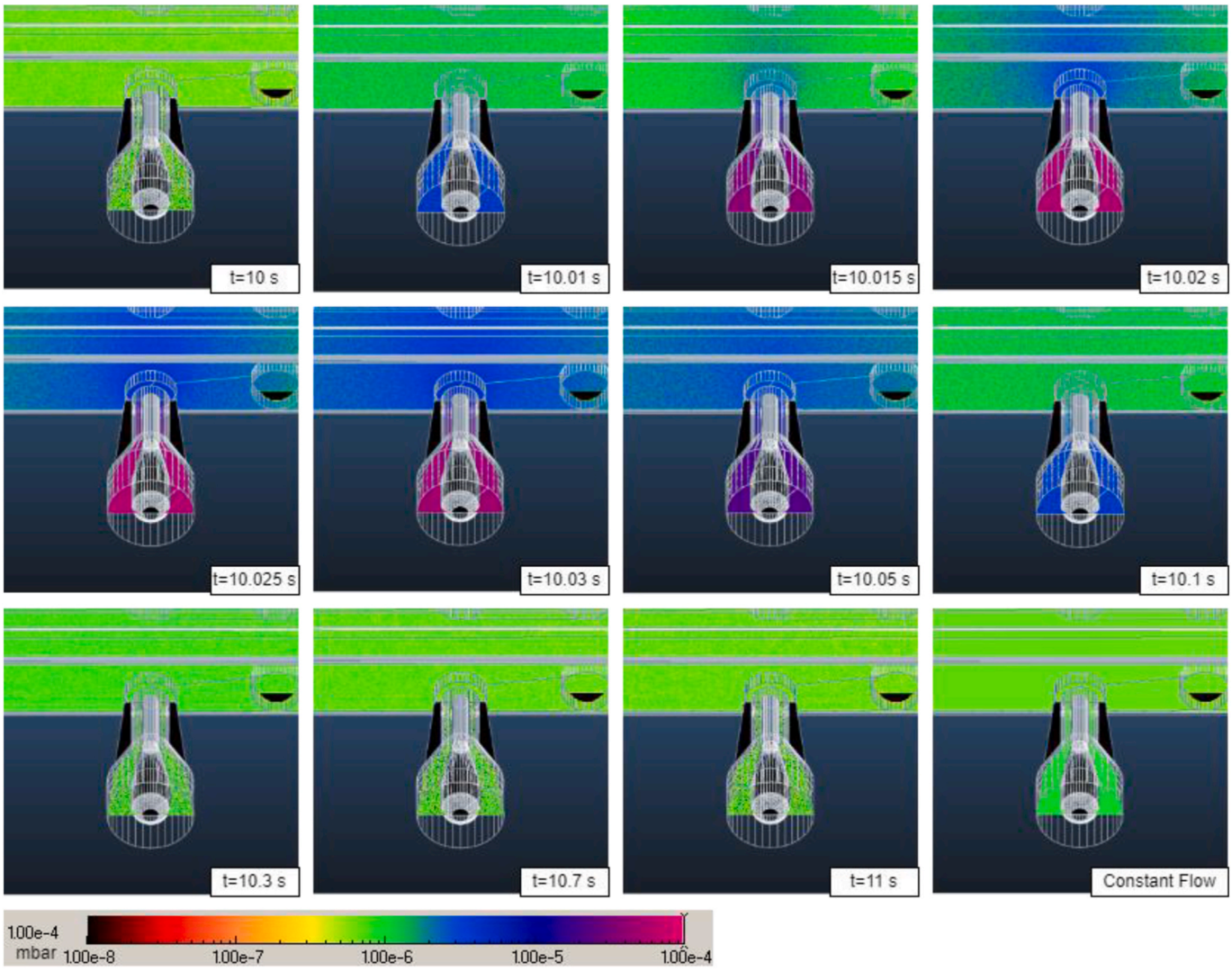

Fig. 18. Transient pressure rise due to a virtual injection of gases emulating an electric arc in the couplers of the RFQ of LIPAc. (t = 10s is when the event occurs).

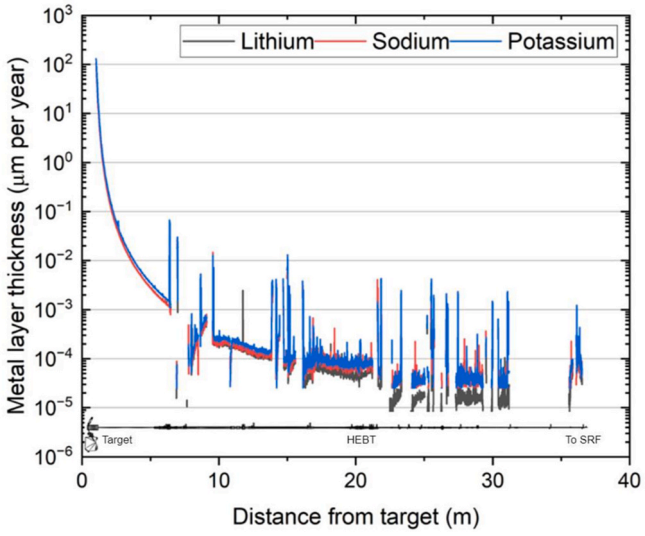

Fig. 19. Metal layer thickness of lithium, sodium and potassium after one year of operation.

Target System and the Accelerator System, located physically inside the Test Cell and compromising a mechanical flanged connection between two rectangular pipe ducts.

The prototype currently undergoing the first experimental campaign is composed of a welded edge bellow section to allow the separation of the two flanges and to compensate for thermal expansions and possible positioning misalignments. This circular below is compressed and expanded by means of a special maneuvering system named One Point Mechanism (OPM), which can be easily operated from a single vertical point simplifying the required remote handling operations.

This OPM system is essentially an assembly consisting of a bevel gear block, which is a mechanism that utilizes bevel gears (with conically shaped teeth) to secure or control the movement of components, often in mechanical systems where precise angular locking or positioning is required; two side screw spindles and two flexible shafts. Finally, a clamping chain and two tightening shafts are included. The sealing of this articulated collar clamp is achieved by means of a spring energized metal gasket, with a built-in retaining system, to prevent detachment during coupling and uncoupling of the flanges. The flanges incorporate a self-centering lip system for male-female insertion.

After passing Factory Acceptance Tests (FAT) the QDS prototype has been sent to the collaborating laboratory, belonging to the Italian research agency ENEA, to carry out multiple tests of manipulation and operation by remote handling, to gain more insight into vacuum,

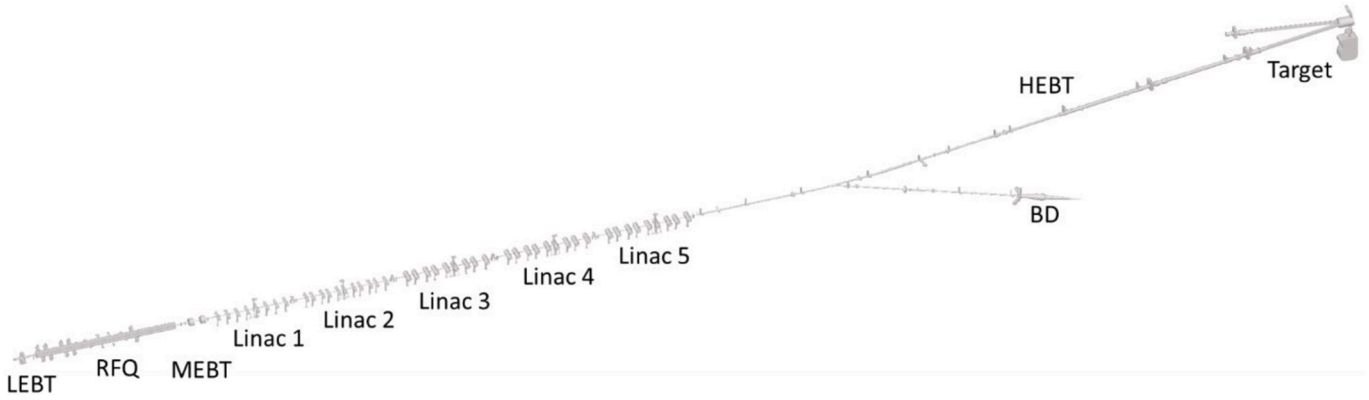

Fig. 20. 3D model used in the complete simulation of the particle accelerator.

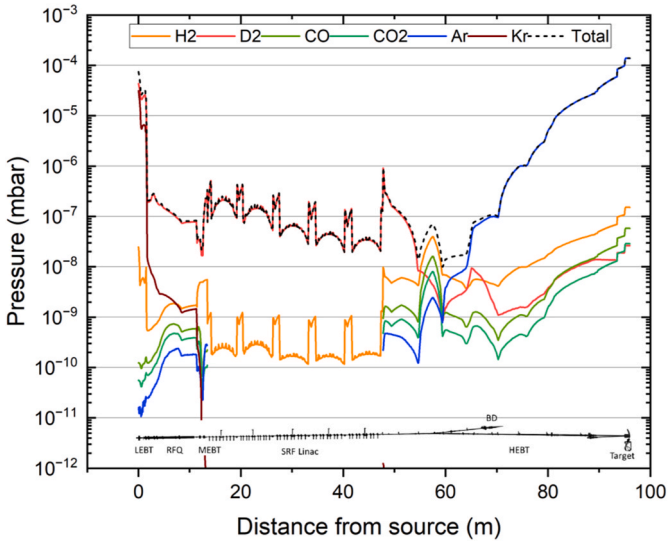

Fig. 21. Gas pressure profile for deuterium (mainly beam losses), hydrogen, carbon monoxide, carbon dioxide (thermal outgassing), argon and krypton injection and total pressure in the IFMIF-DONES accelerator at beam operation (beam goes to target).

mechanical and dynamic performance and behavior. Fig. 24 shows a 3D model of the prototype and Fig. 25 shows the manufactured prototype.

5. Conclusions

The IFMIF-DONES represents an advancement in fusion research, designed to address critical challenges in material testing for future fusion reactors.

The detailed design and operational strategies for IFMIF-DONES, including its advanced particle accelerator and, hence, its complex vacuum system, underscore the importance of maintaining high vacuum levels to ensure optimal beam transport and system performance. Each component of the accelerator—from the Injector to the HEBT section—requires specific vacuum conditions to operate effectively. The comprehensive vacuum system, divided into multiple subsections with specific pressure requirements, is crucial for managing the beam and mitigating the impact of gas loads from various sources.

The ongoing work, including vacuum modeling and the development of prototypes such as the MuVacAS and the QDS, highlights the proactive measures being taken to validate and refine the vacuum system design. These prototypes are instrumental in testing and optimizing strategies for handling vacuum loss incidents and remote handling needs, ensuring the system's reliability and robustness.

In summary, IFMIF-DONES is poised to make significant contributions to the field of fusion energy by providing essential data on material behavior under neutron irradiation. The meticulous design and testing of its vacuum system are fundamental to its success, demonstrating the

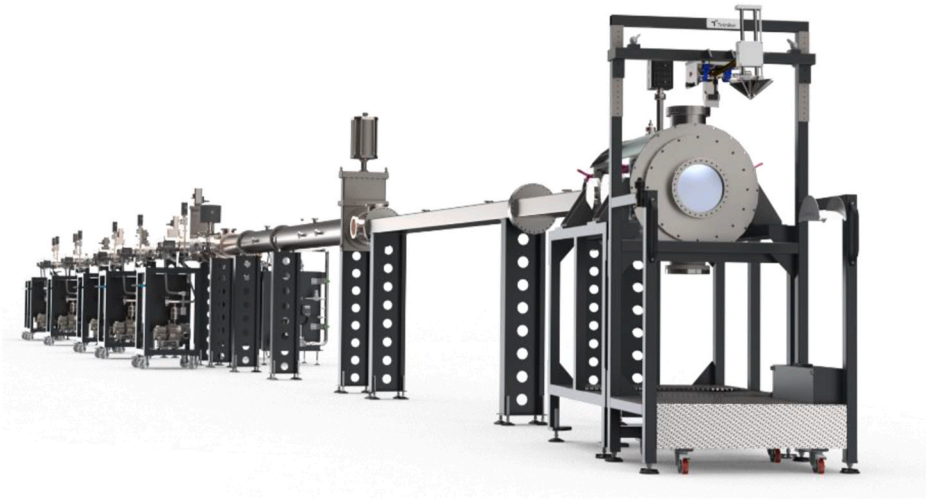

Fig. 22. 3D model of MuVacAS.

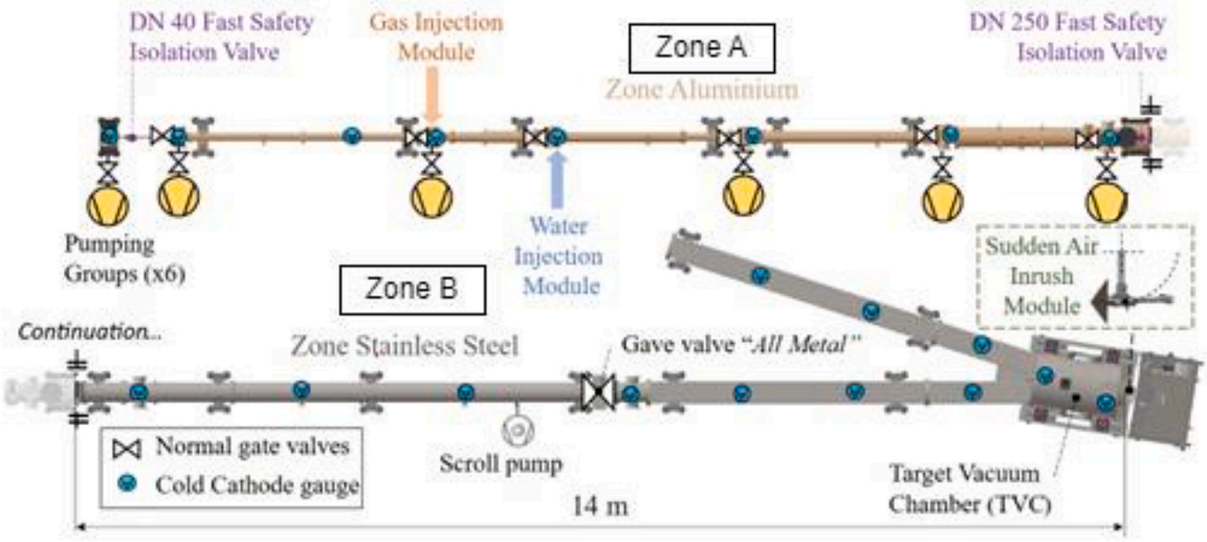

Fig. 23. Simplified schematic of MuVacAS.

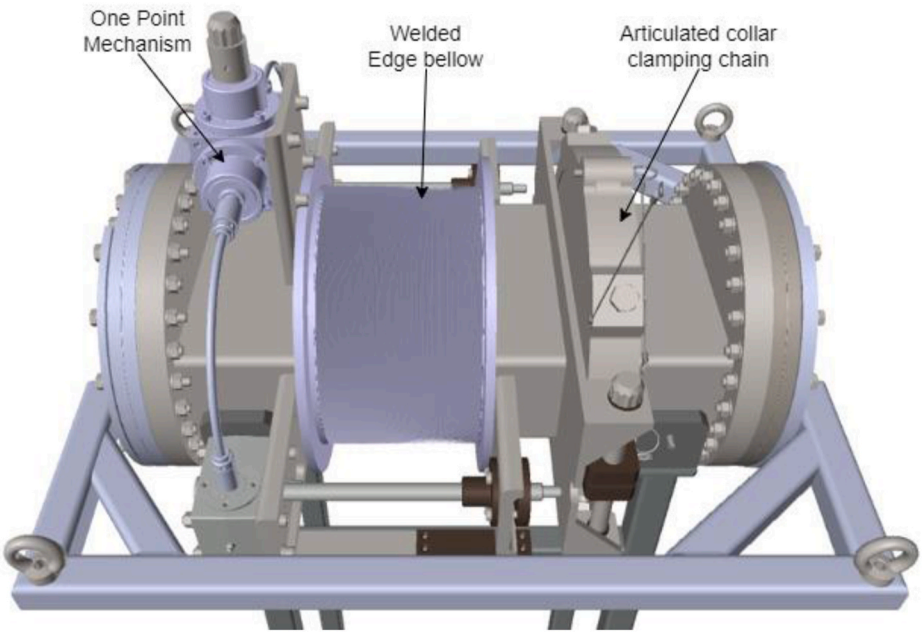

Fig. 24. 3D model of QDS.

facility's commitment to advancing fusion technology and supporting the broader goal of achieving sustainable and clean energy.

CRediT authorship contribution statement

César Caballero Pérez: Writing – review & editing, Writing – original draft, Visualization, Validation, Resources, Methodology, Funding acquisition, Formal analysis, Data curation, Conceptualization. **Marcelo Juni Ferreira:** Writing – review & editing, Supervision, Conceptualization. **Volker Hauer:** Writing – review & editing, Formal analysis, Conceptualization. **Iván Podadera:** Writing – review & editing, Supervision, Conceptualization. **Anderson Sabogal:** Writing – review & editing, Conceptualization. **Daniel Sánchez Herranz:** Writing – review & editing, Visualization, Conceptualization. **Claudio Torregrosa:** Writing – review & editing, Conceptualization.

Funding

This work has been carried out within the framework of the EUROfusion Consortium, funded by the European Union via the Euratom Research and Training Programme (Grant Agreement No 101052200 — EUROfusion). Views and opinions expressed are however those of the author(s) only and do not necessarily reflect those of the European Union or the European Commission. Neither the European Union nor the European Commission can be held responsible for them.

Declaration of competing interest

The authors declare the following financial interests/personal relationships which may be considered as potential competing interests: Cesar Caballero Perez reports financial support was provided by European Consortium for the Development of Fusion Energy. If there are other authors, they declare that they have no known competing financial

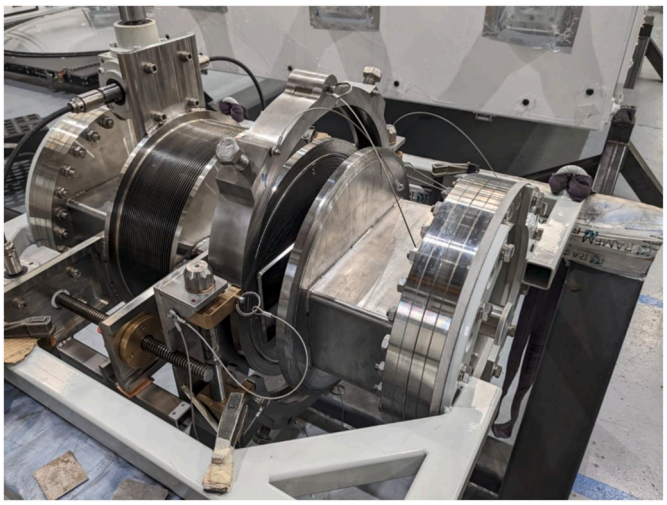

Fig. 25. Prototype of QDS

interests or personal relationships that could have appeared to influence the work reported in this paper.

Data availability

No data was used for the research described in the article.

References

[1] D. Bernardi, et al., The IFMIF-DONES project: design status and main achievements within the EUROfusion FP8 work Programme, J. Fusion Energy 41 (2) (Dec. 2022), https://doi.org/10.1007/s10894-022-00337-5.

[2] J. Knaster, et al., The accomplishment of the Engineering Design Activities of IFMIF/EVEDA: the European-Japanese project towards a Li(d,xn) fusion relevant neutron source, Nucl. Fusion 55 (8) (Aug. 2015), https://doi.org/10.1088/0029-5515/55/8/086003.

[3] I. Podadera, et al., The accelerator system of IFMIF-DONES multi-MW facility. Proceedings of IPAC2021, 2021, pp. 1910–1913, https://doi.org/10.18429/JACoW-IPAC2021-TUPAB211.

[4] A. Pisent, et al., IFMIF-EVEDA RFQ design, in: Proceedings of EPAC08, 2008. Genoa.

[5] I. Podadera, et al., MANUFACTURING, assembly and tests of the LIPAC medium energy beam transport line (MEBT), in: Proceedings of LINAC2016, East Lansing, MI, USA, 2017.

[6] T. Plomion, et al., Preliminary design of the IFMIF-DONES superconducting LINAC, in: Proceedings of SRF2019, Dresden, Germany, 2019, https://doi.org/10.18429/JACoW-SRF2019-MOP097.

[7] O. Nomen, et al., Preliminary design of the HEBT of IFMIF DONES, Fusion Eng. Des. 153 (Apr. 2020), https://doi.org/10.1016/j.fusengdes.2020.111515.

[8] D. Sánchez-Herranz, et al., Status of the engineering design of the IFMIF-DONES high energy beam transport line and beam dump system, J Phys Conf Ser 2420 (1) (2023), https://doi.org/10.1088/1742-6596/2420/1/012080.

[9] L. Macià, et al., Engineering design status of IFMIF-DONES high energy beam transport line and beam dump system inside the TIR and RIZ, Fusion Eng. Des. 202 (May 2024) 114312, https://doi.org/10.1016/J.FUSENGDES.2024.114312.

[10] V. Hauer, C. Day, IFMIF-DONES gas flow modelling [Online]. Available: http://www.euro-fusionscipub.org. (Accessed 8 August 2024).

[11] V. Hauer, C. Day, A preliminary assessment of the vacuum performance in the beamline during IFMIF-DONES operation, Fusion Eng. Des. 136 (Nov. 2018) 1063–1067, https://doi.org/10.1016/j.fusengdes.2018.03.038.

[12] C.C. Perez, F. Scantamburlo, A. De Franco, I. Moya, L. Gonzalez-Gallego, J. M. Garcia, Transient vacuum study of electric arc in Radio frequency Quadrupole of the linear particle accelerator IFMIF, Proceed. Int. Sympo. Discharg. Electri. Insul Vacu. ISDEIV 2023-June (2023) 322–325, https://doi.org/10.23919/ISDEIV55268.2023.10199604.

[13] T. Kanemura, H. Kondo, T. Furukawa, Y. Hirakawa, E. Wakai, J. Knaster, Analytical and experimental study of the evaporation and deposition rates from a high-speed liquid lithium jet, Fusion Eng. Des. 122 (2017), https://doi.org/10.1016/j.fusengdes.2017.08.020.

[14] P. Kneisel, Effect of cavity vacuum on performance of superconducting niobium cavities, in: Proceedings of the 1995 Workshop on RF Superconductivity, Gif-Sur-Yvette, France, 1995. Accessed: Dec. 13, 2024. [Online]. Available: https://accelconf.web.cern.ch/SRF95/papers/srf95c16.pdf.

[15] A. Sabogal, C. Torregrosa-Martín, D. Rodríguez, MULTIPURPOSE VACUUM ACCIDENT SCENARIOS (MUVACAS) PROTOTYPE FOR THE IFMIF-DONES LINEAR ACCELERATOR, 2022, https://doi.org/10.18429/JACoW-IPAC2023-THPA156.